JOURNAL OF THERMOPHYSICS AND HEAT TRANSFER
Vol. 9, No. 3, July–September 1995

# Thermal Response of Thin-Film High-$T_c$ Superconductors to Modulated Irradiation

Patrick E. Phelan*
*University of Hawaii at Manoa, Honolulu, Hawaii 96822*

**A one-dimensional analytical thermal model applied to thin-film high-$T_c$ superconductors provides a convenient technique for calculating the bolometric response of these films to modulated irradiation. Significant features of the model include modulated radiative heating of the film, film/substrate and substrate/cold finger thermal boundary resistances, and Joule heating within the film. The calculated voltage response is in qualitative agreement with measured data, and exhibits the same trends as the data for all calculated frequencies. In a parametric study, the effects of varying substrate/cold finger thermal boundary resistance and substrate thickness are shown to be especially significant with regard to the responsivity at low frequencies.**

## Nomenclature

$A$ = contact area, $m^2$
$a_f$ = film radiative absorptance
$c$ = specific heat, J $kg^{-1}$ $K^{-1}$
$D$ = substrate thickness, mm
$d$ = film thickness, nm
$E$ = dimensionless constant, Eq. (14)
$Fo$ = Fourier number
$f$ = radiation modulation frequency, Hz
$G$ = thermal conductance, W $K^{-1}$
$h$ = width of the high-$T_c$ bridge, m
$I$ = bias current, A
$J$ = bias current density, A $m^{-2}$
$k$ = thermal conductivity, W $m^{-1}$ $K^{-1}$
$L$ = length of the high-$T_c$ bridge, m
$N$ = complex refractive index
$Q$ = dimensionless constant, Eq. (10)
$q_i$ = incident radiative heat flux, W $m^{-2}$
$R$ = thermal resistance, $m^2$ K $W^{-1}$
$R_{tot}$ = total thermal resistance, K $W^{-1}$
Re = real part
$r$ = electrical resistivity, Ω m
$T$ = temperature, K
$t$ = time, s
$z$ = position coordinate
$\Gamma_1$, $\Gamma_2$ = dimensionless constants, Eq. (10)
$\gamma$ = dimensionless constant, Eq. (10)
$\Delta T$ = temperature increase, K
$\Delta V$ = voltage increase, V
$\eta$ = dimensionless constant, Eq. (14)
$\theta$ = dimensionless temperature
$\tau$ = dimensionless time
$\Phi_1$, $\Phi_2$ = dimensionless constants, Eq. (14)
$\psi$ = dimensionless complex temperature
$\Omega$ = dimensionless constant, Eq. (14)
$\omega$ = angular frequency, rad $s^{-1}$

*Subscripts*
*ac* = periodic component
*b* = film/substrate interface
cu = substrate/Cu interface
*dc* = nonperiodic component
*f* = film
*s* = substrate
0 = initial

*Superscript*
* = dimensional variable

Received May 16, 1994; presented as Paper 94-2080 at the AIAA/ASME 6th Joint Thermophysics and Heat Transfer Conference, Colorado Springs, CO, June 20–23, 1994; revision received Nov. 21, 1994; accepted for publication Nov. 22, 1994. 

*Assistant Professor, Department of Mechanical Engineering, 2540 Dole St. Member AIAA.

## Introduction

THIN-FILM high-$T_c$ (high-critical temperature) superconductors are widely advocated to be used as the sensing element in infrared (IR) and far-IR bolometers.[1,2] Their voltage response to incident radiation comes about through two mechanisms: 1) a bolometric, or thermal, mechanism, and 2) a nonbolometric, or nonthermal, mechanism. The bolometric mechanism is due to an increase in the film temperature caused by the irradiation, which results in a detectable change in the temperature-dependent electrical resistivity of the film. The nonbolometric mechanism is based on the nonequilibrium quasiparticle density that can be induced by the irradiation. In this study, a thermal analysis of the bolometric response is applied to a system composed of a high-$T_c$ thin film on a substrate, which is illuminated by modulated or chopped, continuous-wave (cw) irradiation. The goal of the investigation is to provide a relatively simple, yet accurate, thermal model that can be used to enhance the design of high-$T_c$ radiation detectors. More comprehensive numerical models on the voltage response to pulsed[3–5] and cw[5] irradiation have been presented earlier. Here, a one-dimensional analytical thermal model, based on the classical Fourier equation, is employed that considers the film/substrate and substrate/cold finger thermal boundary resistances, radiative absorption and Joule heating within the film, and thermal conduction in the substrate. The calculated voltage response is compared with experimental data,[6] in which a meander-patterned Y-Ba-Cu-O film on a $LaAlO_3$ substrate was irradiated with a light-emitting diode (LED) that produced incoherent radiation with a peak wavelength at 0.85 μm, and which was modulated with a fixed square-wave driving current. It was found[6] that the measured voltage response deviated from that calculated using a simple thermal model that assumed a constant value of $G$, the overall thermal conductance between the film and the environment, for modulation frequencies $f$ above about 30 Hz. However, it has been shown that $G$ can vary strongly with $f$ for a high-$T_c$ microbolometer,[7] thus impacting the predicted voltage response. The present analytical model makes no such assumptions about $G$, and thus is able to more ac-

curately predict the high-frequency thermal voltage response of the high-$T_c$ film.

## Thermal Model

A schematic diagram of the meander pattern employed in the previous experimental study[6] is presented in Fig. 1a. The voltage and current taps are not shown. The total length of the Y-Ba-Cu-O bridge $L$ is 3.358 cm, the width $h$ is 90 $\mu$m, and the spacing between the lines is 150 $\mu$m. The entire meander pattern is uniformly irradiated with the LED positioned approximately 1.5 cm from the sample.

Figure 1b is an expanded isometric view of the central portion of the meander pattern demarcated in Fig. 1a. The film thickness $d$ is 550 nm, and the substrate thickness $D$ is 0.5 mm. The sample is cooled by conduction to a Cu cold finger at the base of the substrate, with the rest of the sample exposed to vacuum. The system is modeled as the one-dimensional configuration shown in Fig. 2, which enables a relatively simple analytic solution to be derived. The incident radiative heat flux $q_i$ is assumed to be absorbed only within the film, with a film absorptance $a_f$. The value for $a_f$ is calculated using planar geometric optics, which is appropriate considering the incoherent nature of the source. The geometry for calculating $a_f$ is the same as that of Fig. 2, i.e., a two-layer planar structure bounded on both sides by semi-infinite media. The refractive indices at 0.85 $\mu$m of the film $N_f$, the substrate $N_s$, and of the Cu cold finger $N_{cu}$ are assigned the following values: $N_f = 1.401 + 0.260i$[8]; $N_s = 2.098 + 0.012i$[9]; and $N_{cu} = 0.270 + 5.442i$.[10] The medium above the film is vacuum, with a refractive index of $1 + 0i$. For the given dimensions of $d = 550$ nm and $D = 0.5$ mm, $a_f$ is 0.849.

The principal features of the model are one-dimensional transient thermal conduction within the substrate, a "lumped" film, periodic radiative heating within the film, Joule heating within the film, and thermal boundary resistance between the film and substrate $R_b$ and between the substrate and Cu cold finger $R_{cu}$. In nondimensional form, the one-dimensional substrate heat conduction equation is

$$\frac{\partial \theta_s}{\partial \tau} = Fo \frac{\partial^2 \theta_s}{\partial z^2} \tag{1}$$

where $\theta_s$ is the substrate temperature, $\tau$ time, $Fo$ the Fourier number, and $z$ the spatial coordinate (see Fig. 2). The definitions of these variables are given as follows:

$$\theta_s = (T_s - T_0)/T_0, \quad \tau = \omega t, \quad z = z^*/D, \quad Fo = \alpha_s/\omega D^2 \tag{2}$$

in which the subscript 0 means the initial condition, $\omega = 2\pi f$ the angular frequency of the modulation, $t$ the dimensional time, $\alpha_s$ the substrate thermal diffusivity, * signifies a dimensional variable, and the subscript $s$ represents the substrate.

Equation (1) is subject to the following boundary conditions. At the film/substrate interface ($z = 1$)

$$\frac{\partial \theta_s}{\partial z} = \frac{D}{k_s R_b} [\theta_f - \theta_s (z = 1)] \tag{3}$$

where $k_s$ is the substrate thermal conductivity, and $\theta_f$ the nondimensional film temperature, which is governed by the film energy equation:

$$\frac{d\theta_f}{d\tau} = \frac{a_f q_i(\tau)}{d\rho_f c_f T_0 \omega} + \frac{r_0 J^2}{\rho_f c_f T_0 \omega} + \frac{\left(\frac{dr}{dT}\Big|_{T=T_0}\right) J^2}{\rho_f c_f \omega} \theta_f - \frac{1}{d\rho_f c_f \omega R_b} [\theta_f - \theta_s (z = 1)] \tag{4}$$

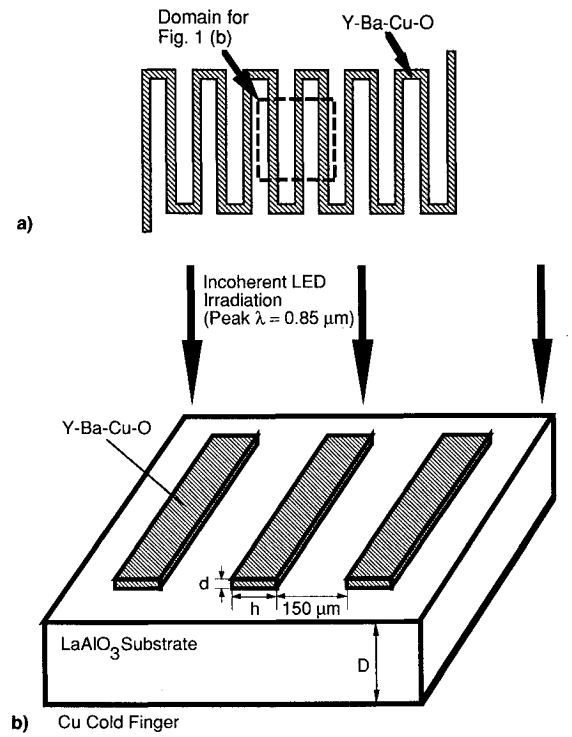


**Fig. 1 a) Etching pattern and b) film and substrate employed in the experimental study.[6]**

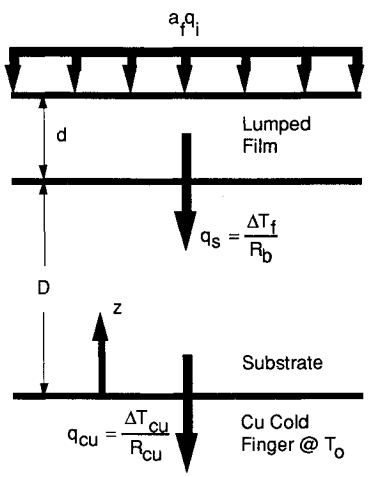


**Fig. 2 Schematic diagram of the thermal model.**

where $\rho_f$ and $c_f$ are the film density and specific heat, $r_0$ the film electrical resistivity at $T_0$, $dr/dT|_{T=T_0}$ the film temperature derivative of $r$ at $T_0$, and $J$ the bias current density. In Eq. (4), the Joule heating in the film has been linearized via

$$rJ^2 \cong \left[r_0 + \left(\frac{dr}{dT}\Big|_{T=T_0}\right)(T_f - T_0)\right] J^2 \tag{5}$$

thus permitting an analytical solution to the problem. The incident radiative heat flux $q_i(\tau)$ is a square wave modulated at frequency $f$, and has a peak amplitude of 21.3 W m$^{-2}$.

At the substrate/Cu interface ($z = 0$)

$$\frac{\partial \theta_s}{\partial z} = \frac{D}{k_s R_{cu}} \theta_s \tag{6}$$

where the Cu cold finger temperature is assumed to remain constant at $T_0$, the initial temperature for both the film and the substrate.

### Thermal Boundary Resistances

The film/substrate thermal boundary resistance $R_b$ has been measured for various high-$T_c$ films and substrates.[11-13] For the temperatures considered in this study, where $T_0 = 79.5$ K, $R_b$ is approximately constant at $10^{-7}$ m$^2$ K W$^{-1}$.

The substrate/Cu thermal boundary resistance is determined primarily by the thickness of the vacuum grease layer between the substrate and the cold finger.[6] The measured thermal conductivity of Apiezon $N$ grease at 100 K of $\approx$0.1 W m$^{-1}$ K$^{-1}$,[14] and assuming a thickness of 0.1 mm, yields $R_{cu} = 10^{-3}$ m$^2$ K W$^{-1}$. For steady-state, *dc* conditions, the total thermal resistance $R_{tot}$ (in K/W) can be represented as

$$R_{tot} = \frac{R_b}{A_f} + \frac{D}{k_s A_s} + \frac{R_{cu}}{A_s} \tag{7}$$

where $A_f$ and $A_s$ are the film and substrate contact areas, respectively. The inverse of $R_{tot}$ is $G$, the overall thermal conductance. Taking $A_f = h \times L = 3.022 \times 10^{-6}$ m$^2$ and $A_s = 5.0 \times 10^{-5}$ m$^2$, the entire substrate area, yields $G = 49$ mW/K. However, the actual substrate area involved in the heat conduction path will be less than the total area, so that this value of $G$ represents an upper bound. Taking $A_s = A_f$ yields a lower bound of $G = 3$ mW/K. These values are compared with the measured[6] one of $G = 8.2$ mW/K.

These values are applicable only for steady-state, *dc* heating of the film, such as that generated by Joule heating with no irradiation. As the film undergoes periodic irradiation, $G$ will increase with increasing frequency, as demonstrated previously[7] and in the following results. The value of $R_{cu} = 10^{-3}$ m$^2$ K W$^{-1}$ is assumed valid for the range of calculated frequencies ($10^{-2}$–$10^6$ Hz), and is considered to be independent of temperature. For this particular experiment,[6] $R_{cu}$ is the dominant resistance to heat conduction from the film.

### Thermophysical and Electrical Properties

The thermophysical properties are taken to be constant at the values corresponding to the initial temperature ($T_0 = 79.5$ K), since the temperature rise caused by the irradiation and Joule heating is less than 1 K. For Y-Ba-Cu-O, using the property functions determined earlier,[4] yields $\rho_f = 6350$ kg m$^{-3}$ and $c_f = 162$ J kg$^{-1}$ K$^{-1}$. The thermal conductivity $k_f$ is not needed in the analysis because the film is assumed to be lumped.

For $LaAlO_3$, $\rho_s = 6520$ kg/m$^3$.[15] The volumetric specific heat $\rho_s c_s$ of this particular sample[6] was determined to be $5.9 \times 10^5$ J K$^{-1}$ m$^{-3}$, thus yielding $c_s = 90.5$ J kg$^{-1}$ K$^{-1}$. The thermal conductivity $k_s$, at 79.5 K, is 26.2 W m$^{-1}$ K$^{-1}$.[16]

Although Eq. (4) includes the initial electrical resistivity, $r_o$, during periodic heating only the temperature derivative $dr/dT|_{T=T_0}$ is important. As given in the experimental study,[6] $dR/dT|_{T=T_0}$ is 672 Ω K$^{-1}$ for this sample, yielding $dr/dT|_{T=T_0} = 9.9 \times 10^{-7}$ Ω m K$^{-1}$. The derivative $dR/dT|_{T=T_0}$ was reported to be independent of bias current for currents significantly less than the sample critical current.[6]

### Solution

The solution for $\theta_f$ can be separated into a *dc*, or steady-state, nonperiodic component, and an *ac*, or steady-state, periodic component.[7] The radiative input is correspondingly written as the sum of a *dc* component and an *ac* component

$$a_f q_i = \frac{a_f q_i}{2} + \frac{a_f q_i}{2}\cos(\tau) \tag{8}$$

where the incident square wave is modeled as a sinusoid for simplicity.

The solution for the *dc* component $\theta_{f,dc}$ is straightforward and is expressed as

$$\theta_{f,dc} = \frac{(Q + \Gamma_1)[1 + \gamma + (R_{cu}/R_b)]}{1 - \Gamma_2[1 + \gamma + (R_{cu}/R_b)]} \tag{9}$$

where

$$Q = \frac{a_f q_i R_b}{2T_0}, \quad \gamma = \frac{D}{k_s R_b}, \quad \Gamma_1 = \frac{dR_b J^2 r_0}{T_0}$$
$$\Gamma_2 = dR_b J^2 \left(\frac{dr}{dT}\bigg|_{T=T_0}\right) \tag{10}$$

Thus, $Q$ represents the radiative input, $\Gamma_1$ the initial Joule heating, and $\Gamma_2$ the additional Joule heating incurred during the film temperature increase. Note that if it is desired to learn the film temperature rise due to Joule heating only (i.e., $q_i = 0$), take $Q = 0$ in the previous expression.

A complex representation for $\theta_f$ is employed to determine the *ac* component $\theta_{f,ac}$, such that

$$\theta_{f,ac} = \mathrm{Re}[\psi_f] \tag{11}$$

where $\psi_f$ is the complex temperature. Assuming the solution for $\psi_f$ is in the form

$$\psi_f = \psi_{f0} e^{i\tau} \tag{12}$$

where $i = \sqrt{-1}$, the resulting expression for $\psi_{f0}$ is

$$\psi_{f0} = \left\{\frac{\Phi_1 e^{\eta} - E\Phi_2 e^{-\eta}}{(\Omega i - \Gamma_2 + 1)[\Phi_1 e^{\eta} - E\Phi_2 e^{-\eta}] - \gamma\sqrt{2Fo}(e^{\eta} + Ee^{-\eta})}\right\} Q \tag{13}$$

where

$$\eta = \frac{1+i}{\sqrt{2Fo}}, \quad \Omega = d\rho_f c_f \omega R_b, \quad \Phi_1 = 1 + i + \gamma\sqrt{2Fo}$$
$$\Phi_2 = 1 + i - \gamma\sqrt{2Fo}, \quad E = \frac{(1+i)k_s R_{cu} - D\sqrt{2Fo}}{(1+i)k_s R_{cu} + D\sqrt{2Fo}} \tag{14}$$

and then the peak film temperature rise $\Delta T_{f,ac} = T_{f,ac} - T_0$ is found from

$$\Delta T_{f,ac} = T_0 \,\mathrm{Re}[\psi_{f0}] \tag{15}$$

## Results and Discussion

A comparison between the calculated voltage response $\Delta V_c$ and the measured voltage response $\Delta V_m$ is given in Fig. 3. For this and the following graphs, $d = 550$ nm and $R_b = 10^{-7}$ m$^2$ K W$^{-1}$, with the other parameters reported in the figure captions. The calculated voltage response is determined from

$$\Delta V_c = I \left.\frac{dR}{dT}\right|_{T=T_0} \Delta T_{f,ac} \tag{16}$$

where $I$ is the *dc* bias current. Also shown for comparison is the result of the previous model presented with the experimental data,[6] in which the *dc* value of $G$ is applied for all frequencies. It is readily apparent that for higher frequencies, the present theoretical results more closely match the experimental data, even though a relatively simple one-dimensional model has been assumed. Multidimensional effects may become more significant when the frequency-dependent thermal penetration depth[17] $\delta$ in the substrate, calculated from

$$\delta = \sqrt{\alpha_s/\pi f} \tag{17}$$

becomes comparable with one-half the spacing between the meander lines (Fig. 1). This occurs around $1.5 \times 10^3$ Hz for

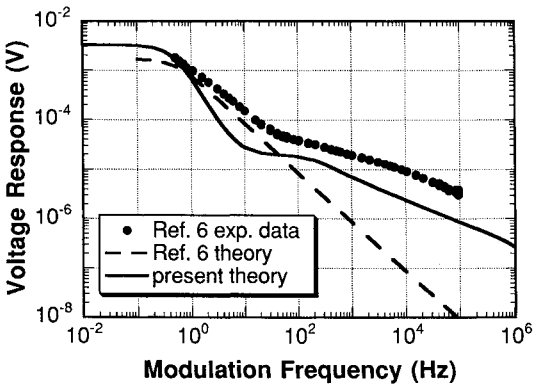


**Fig. 3 Comparison between experimental and calculated results ($D$ = 0.5 mm, $I$ = 500 $\mu$A, $R_{cu}$ = $10^{-3}$ m$^2$ K W$^{-1}$).**

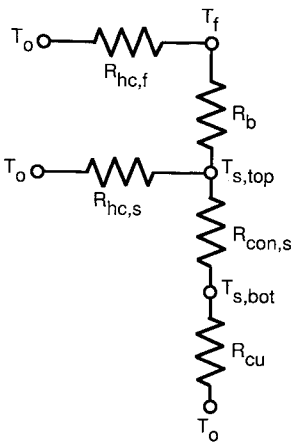


**Fig. 4 Equivalent thermal resistance network.**

the $LaAlO_3$ substrate, and may explain the slight change in slope in the experimental data of Fig. 3 between $10^3$–$10^4$ Hz.

Both the experimental data and the present theory show a distinct change of slope in the voltage response between $10^1$–$10^2$ Hz, a feature which is not indicated by the earlier model. The explanation lies in the frequency dependence of $G$.

An approximate equivalent thermal resistance network is presented in Fig. 4 that includes frequency-dependent effects. The film node, or temperature $T_f$, is shown at the upper right portion of the diagram. The other temperatures are the substrate temperature adjacent to the film/substrate interface ($T_{s,\text{top}}$), the substrate temperature adjacent to the substrate/Cu interface ($T_{s,\text{bot}}$), and the initial temperature $T_0$. The thermal resistances $R_{hc,f}$ and $R_{hc,s}$ are the resistances due to the film and substrate heat capacities, respectively. These resistances are derived by considering the transient term in the energy equation. For example, in the film we have

$$d\rho_f c_f \frac{\partial T_f}{\partial t} = q_{hc,f} = \frac{\Delta T_f}{R_{hc,f}} \tag{18}$$

where $q_{hc,f}$ is the heat flux being absorbed by the film heat capacity. If the temperature derivative is scaled as

$$\frac{\partial T_f}{\partial t} \sim \omega \Delta T_f \tag{19}$$

then for $R_{hc,f}$ we have

$$R_{hc,f} \sim 1/d\rho_f c_f \omega \tag{20}$$

A similar expression is derived for $R_{hc,s}$. However, in this case $\delta$ must also be considered, yielding

$$R_{hc,s} \cong \begin{cases} 1/D\rho_s c_s \omega, & D < \delta \\ 1/\delta\rho_s c_s \omega, & \delta < D \end{cases} \tag{21}$$

For $dc$ heating where $\omega = 0$, $R_{hc,f}$ and $R_{hc,s}$ are both infinite, leaving the traditional $dc$ thermal resistance network of $R_b$, $R_{con,s}$, and $R_{cu}$.

For low frequencies less than about $2 \times 10^{-1}$ Hz, $\Delta V_c$ is almost flat. At these frequencies, $R_{hc,f}$ and $R_{hc,s}$ are so large that these paths are effectively open circuits, so that all the heat flow proceeds from $T_f$ vertically downward to $T_0$. A comparison of the magnitudes of $R_b$, $R_{con,s}$, and $R_{cu}$ shows that $R_{cu}$ is the dominating resistance at $10^{-3}$ m$^2$ K W$^{-1}$. Since $R_{cu}$ remains constant, the effective thermal resistance between $T_f$ and $T_0$ remains constant, and hence, the constant $\Delta V_c$.

Around $f \approx 2 \times 10^{-1}$ Hz, $R_{hc,s}$ becomes comparable to $R_{cu}$ (of order $10^{-3}$ m$^2$ K W$^{-1}$), so that now some of the heat flux passes through $R_{hc,s}$. From Eq. (21), $R_{hc,s}$ decreases with increasing $f$, and thus the effective resistance between $T_f$ and $T_0$ decreases, resulting in the decrease in $\Delta V_c$.

Another relatively flat region occurs for $\Delta V_c$ for $10^1 < f < 10^2$ Hz. In this frequency range $R_{hc,s}$ is comparable to $R_{con,s}$. But, at $10^2$ Hz, $\delta$ becomes comparable with $D$, the substrate thickness. This means that $R_{hc,s}$ is described by the lower expression in Eq. (21), which decreases as $\omega^{-1/2}$. Similarly, since $\delta \leq D$ and the heat flux does not reach the substrate/Cu interface, $R_{con,s}$ is now approximated by

$$R_{con,s} \cong \delta/k_s \tag{22}$$

and "shorts out" $R_{cu}$, which no longer impacts $T_f$. The combined parallel resistance of $R_{con,s}$ and $R_{hc,s}$ is now the limiting resistance, and as it decreases with increasing $f$, so does $\Delta V_c$.

The sources of the discrepancy between $\Delta V_c$ and $\Delta V_m$ are not clear. It was originally anticipated that the one-dimensional model would predict $\Delta V_c > \Delta V_m$, because of the lack of heat spreading in three dimensions. That is obviously not the case. One possible cause for $\Delta V_m < \Delta V_c$ is assuming too high a value for $k_s$. It seems that $c_s$ for this sample is relatively low, compared to published data on $LaAlO_3$.[15] The same may hold true for $k_s$, which would give rise to the underprediction by the present model.

The effect of the bias current $I$ is demonstrated in Fig. 5. Here, the responsivity $S$ is plotted rather than $\Delta V_c$. The responsivity is defined as the voltage response divided by the incident radiative power, and is determined from

$$S = \Delta V_c / q_i h L \tag{23}$$

where $h$ is the film width and $L$ is the film length. From Eq. (16), we expect at least a linear dependence of $\Delta V_c$ on $I$. At

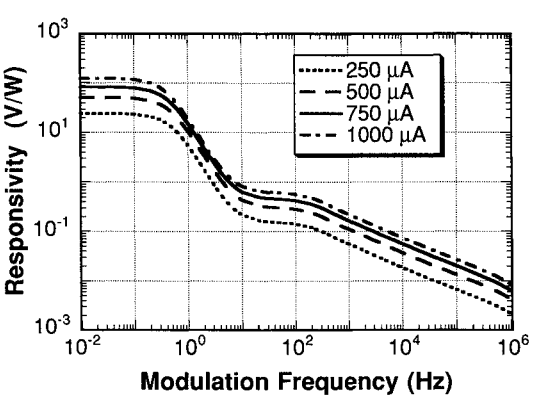


**Fig. 5 Responsivity vs frequency as a function of bias current ($D$ = 0.5 mm and $R_{cu}$ = $10^{-3}$ m$^2$ K W$^{-1}$).**

low frequencies, the Joule heating tends to enhance the effect of $I$, especially at the higher currents. If the Joule heating term is not included, or in other words if $\Gamma_2 = 0$ in Eq. (13), then at low frequencies ($f < 0.6$ Hz) there is a 1% error for $I = 250$ $\mu$A, and up to 23% error for $I = 1000$ $\mu$A. At moderate frequencies ($0.6 < f < 100$ Hz), taking $\Gamma_2 = 0$ actually increases $\Delta V_c$, and then as the frequency is increased further ($f > 100$ Hz) there is almost no effect of neglecting Joule heating.

Figure 6 shows the significant influence of $R_{cu}$ on $S$. As stated above in the discussion of Fig. 3, $R_{cu}$ has no effect on the voltage response for high frequencies where $\delta < D$, a trend visibly demonstrated in Fig. 6. However, as shown there are significant effects at lower frequencies, and depending on the frequency range, increasing $R_{cu}$ may either increase or decrease $S$. For $R_{cu} = 10^{-2}$ m$^2$ W K$^{-1}$, the highest value of $R_{cu}$, from the lowest frequencies $R_{bc,s} \leq R_{cu}$, so that the heat flux passes through $R_{bc,s}$ rather than $R_{cu}$. At intermediate frequencies, $R_{bc,s} \sim R_{con,s}$, and again we have a flat response since the total thermal resistance is relatively constant in this frequency range. Finally, around $f = 10^2$ Hz, $\delta$ becomes less than $D$, giving rise to the monotonic decrease in $S$. At the other extreme where $R_{cu} = 10^{-5}$ m$^2$ W K$^{-1}$, $R_{cu}$ is much smaller than $R_{bc,s}$ at lower frequencies, leading to the flat response until $f \cong 10$ Hz.

The influence of substrate thickness $D$ on $S$ is given in Fig. 7. Note that changing $D$ has no impact on $a_f$. At higher frequencies, all the curves merge into a common, decreasing line, as before. However, in Fig. 7 each curve joins the common curve at different values of $f$, since $\delta = D$ occurs at different frequencies for each $D$. For $D = 0.1$ mm, the smallest value of $D$, $\delta = D$ near $f = 10^3$ Hz, and for $D = 1.0$ mm, $\delta = D$ at $f = 14$ Hz.

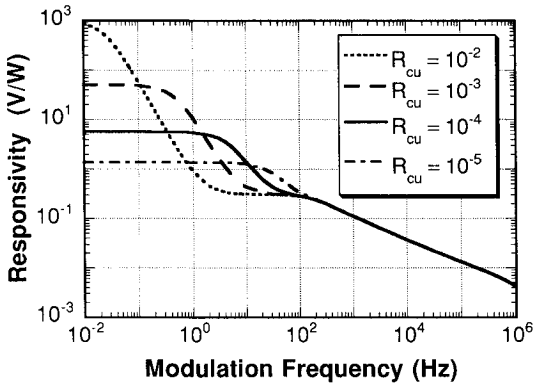


**Fig. 6 Responsivity vs frequency as a function of substrate/Cu thermal contact resistance. $R_{cu}$ is in units of m$^2$ K W$^{-1}$ ($D = 0.5$ mm and $I = 500$ $\mu$A).**

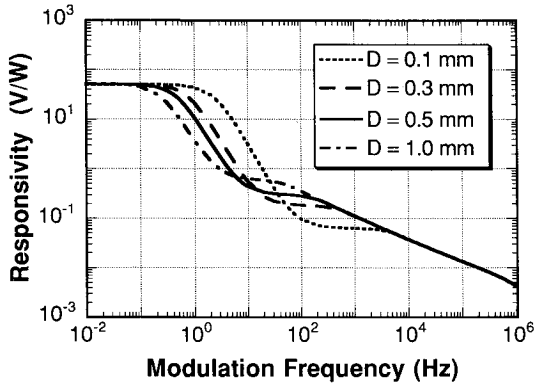


**Fig. 7 Responsivity vs frequency as a function of substrate thickness ($R_{cu} = 10^{-3}$ m$^2$ K W$^{-1}$ and $I = 500$ $\mu$A).**

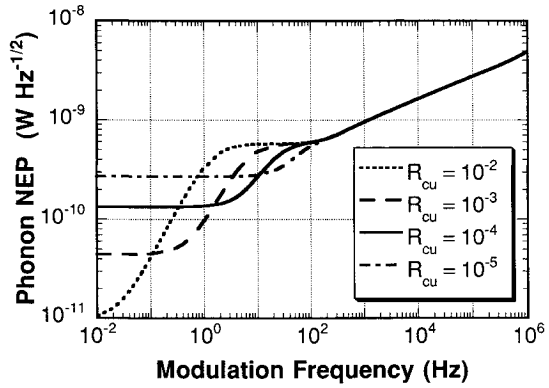


**Fig. 8 Phonon NEP vs frequency as a function of $R_{cu}$. $R_{cu}$ is in units of m$^2$ K W$^{-1}$ ($D = 0.5$ mm and $I = 500$ $\mu$A).**

The final graph is presented in Fig. 8. The noise equivalent power due to thermal fluctuations, or the phonon NEP, is given as a function of $f$, for varying $R_{cu}$. The phonon NEP is the ultimate lower limit for the total NEP, and is calculated from[18]

$$\text{NEP} = T_0\sqrt{4k_bG_{ac}} \tag{24}$$

where $k_b$ is the Boltzmann constant, and $G_{ac}$ is the thermal conductance during periodic radiative heating, and is computed from

$$G_{ac} = \frac{a_f q_i h L}{\Delta T_{f,ac}} \tag{25}$$

The initial temperature $T_0$ is used in Eq. (24) instead of the actual temperature, since $\Delta T_{f,ac}$ is small. The curves in Fig. 8 have trends opposite of those in Fig. 6, since NEP $\propto \sqrt{G_{ac}}$, whereas $S \propto 1/G_{ac}$.

## Conclusions

A one-dimensional analytical thermal model is developed that is capable of predicting the qualitative trends of the voltage response of thin-film high-$T_c$ superconductors to incident modulated radiation. The model takes into account the periodic radiative heating of the film, the film/substrate and the substrate/cold finger thermal boundary resistances, and Joule heating in the film. The calculated responsivities are shown to depend sensitively on the modulation frequency, the thermal boundary resistance between the substrate and the cold finger, and the substrate thickness.

## Acknowledgments

This material is based upon work supported by the National Science Foundation under Grant CTS93-07753. The author expresses his appreciation to A. Rothwarf and M. Fardmanesh of Drexel University, who generously provided information about their experimental data, and to M. Kelkar of the University of Hawaii, who reviewed the manuscript.

## References

[1]Richards, P. L., Clarke, J., Leoni, R., Lerch, Ph., Verghese, S., Beasley, M. R., Geballe, T. H., Hammond, R. H., Rosenthal, P., and Spielman, S. R., "Feasibility of the High-$T_c$ Superconducting Bolometer," *Applied Physics Letters*, Vol. 54, No. 3, 1989, pp. 283–285.

[2]Zhang, Z. M., and Frenkel, A., "Thermal and Nonequilibrium Responses of Superconductors for Radiation Detectors," *Journal of Superconductivity*, Vol. 7, 1994, pp. 871–884.

[3]Flik, M. I., Phelan, P. E., and Tien, C. L., "Thermal Model for the Bolometric Response of High-$T_c$ Superconducting Films to Op

tical Pulses," *Cryogenics*, Vol. 30, No. 6, 1990, pp. 1118–1128.

[4]Phelan, P. E., and Hijikata, K., "Thermal Component of the Optical Response of Thin-Film High-$T_c$ Superconductors," *Journal of the Electrochemical Society*, Vol. 141, No. 3, 1994, pp. 810–815.

[5]Chen, R.-C., Wu, J.-P., and Chu, H.-S., "Bolometric Response of High-$T_c$ Superconducting Detectors to Optical Pulses and Continuous Waves," American Society of Mechanical Engineers Paper 93-HT-7, Aug. 1993.

[6]Fardmanesh, M., Ihsan, M., Scoles, K., and Rothwarf, A., "Thin Film YBCO Infrared Detector Design and Characterization," *6th Annual Conference on Superconductivity and Applications*, American Inst. of Physics Proceeding 273, Buffalo, NY, 1993, pp. 142–154.

[7]Fushinobu, K., Phelan, P. E., Hijikata, K., Nagasaki, T., and Flik, M. I., "Thermal Analysis of the Performance of a High-$T_c$ Superconducting Microbolometer," *Journal of Heat Transfer*, Vol. 116, No. 1, 1994, pp. 275–278.

[8]Kamarás, K., Herr, S. L., Porter, C. D., Tanner, D. B., Etemad, S., and Chan, S.-W., "Optical Excitations in Thin Film $YBa_2Cu_3O_7$," *Progress in High Temperature Superconductivity*, Vol. 17, World Scientific, Singapore, 1989, p. 347.

[9]Calvani, P., Capizzi, M., Donato, F., Dore, P., Lupi, S., Maselli, P., and Varsamis, C. P., "Infrared Optical Properties of Perovskite Substrates for High-$T_c$ Superconducting Films," *Physica C*, Vol. 181, Nos. 4/6, 1991, pp. 289–295.

[10]Palik, E. D., *Handbook of Optical Constants of Solids*, Academic, Orlando, FL, 1985, p. 285.

[11]Nahum, M., Verghese, S., Richards, P. L., and Char, K., "Thermal Boundary Resistance for $YBa_2Cu_3O_{7-\delta}$ Films," *Applied Physics Letters*, Vol. 59, No. 16, 1991, pp. 2034–2036.

[12]Phelan, P. E., Song, Y., Nakabeppu, O., Ito, K., Hijikata, K., Ohmori, T., and Torikoshi, K., "Film/Substrate Thermal Boundary Resistance for an Er-Ba-Cu-O High-$T_c$ Thin Film," *Journal of Heat Transfer*, Vol. 116, No. 4, 1994, pp. 1038–1041.

[13]Phelan, P. E., Song, Y., and Kelkar, M., "Film/Substrate Thermal Boundary Resistance for Er-Ba-Cu-O High-$T_c$ Thin Films," *Grain Boundaries and Interfacial Phenomena in Electronic Ceramics, Ceramic Transactions*, Vol. 41, The American Ceramics Society, Westerville, OH, 1994, pp. 307–314.

[14]Ashworth, T., Loomer, J. E., and Kreitman, M. M., "Thermal Conductivity of Nylons and Apiezon Greases," *Advances in Cryogenic Engineering*, Vol. 18, 1973, pp. 271–279.

[15]Michael, P. C., Trefny, J. U., and Yarar, B., "Thermal Transport Properties of Single Crystal Lanthanum Aluminate," *Journal of Applied Physics*, Vol. 72, No. 1, 1992, pp. 107–109.

[16]Morelli, D. T., "Thermal Conductivity of High Temperature Superconductor Substrate Materials: Lanthanum Aluminate and Neodymium Aluminate," *Journal of Materials Research*, Vol. 7, No. 9, 1992, pp. 2492–2494.

[17]Carslaw, H. S., and Jaeger, J. C., *Conduction of Heat in Solids*, 2nd ed., Oxford Univ. Press, Oxford, England, UK, 1959, p. 263.

[18]Nahum, M., Hu, Q., Richards, P. L., Sachtjen, S. A., Newman, N., and Cole, B. F., "Fabrication and Measurement of High $T_c$ Superconducting Microbolometers," *IEEE Transactions on Magnetics*, Vol. MAG-27, 1991, pp. 3081–3084.